

Study of the effect of microstructure and magnetic texture on major hysteresis loop phenomenology using OOMMF

Mehrija Hasičić, Aphrodite Ktena and Jasna Hivziefendic

Abstract— This paper presents a study of the effect of microstructure and magnetic texture on the hysteresis loop through quasi-static micromagnetic simulations using the open-source software OOMMF. Results show that microstructure and magnetic texture parameters can be used to control the coercivity. The anisotropy constant is the parameter mainly controlling the coercivity. The increase in the volume fraction of hard inclusions in a soft matrix typically leads to higher coercivity. In the case of randomly oriented inclusions, the calculated coercivity is lower than that for the homogeneous soft case which is explained through the prominent anisotropy energy density compared to the much weaker exchange energy density. The results will be used to correlate simulation parameters with magnetic parameters obtained from major hysteresis loop measurements.

Index Terms—micromagnetic calculation, microscopic modeling, energy minimization, magnetic properties, hysteresis loop, OOMMF

I. INTRODUCTION

MAGNETIC materials have played a significant part in the formation of modern civilization and continue to do so in the advancement of industrial and scientific development. Their applications range from the compass, which was the first known application, to power generation and transmission, electronic appliances, analogue and digital data storage, medical appliances such as magnetic resonance imaging (MRI), magnetic therapy, and drug delivery, sensors and actuators, scientific instruments, and so on [1].

Electrical steel, in particular, is a material that is widely used in construction, shipping and other modes of transportation, automobiles, electrical equipment and appliances, and other metallic products. Reducing waste and saving energy is a highly discussed and investigated topic. Increasing efficiency and lifecycle of the electrical machines would be beneficial for both topics.

Stresses are the result of both thermomechanical treatments during the manufacturing of the materials and fatigue during the lifetime of a steel structure. They are difficult to avoid however, they should be monitored and

treated if and when possible [2]. Increased stress levels are known to contribute to losses [3], [4].

The study of the effects contributing to losses as well as the effect of stress on the magnetization process is necessary for the optimization of magnetic materials used in the above applications. Several physical or phenomenological models of magnetization have been developed to assist in the design of new materials or contribute to the control of magnetization driven processes. These models can be grouped into phenomenological [5]–[8], microscopic [9]–[12], atomistic [13], [14] and multiscale [15]–[18].

The modeling of the magnetization process consists in determining the relationship between the magnetization state of a material and external stimuli, such as externally applied fields, mechanical loads, or heating. The major hysteresis loop $M(H)$ of a material, where M represents magnetization of the material and H is applied field, yields the macroscopic parameters typically used to classify a given material, such as the saturation magnetization, remanence, coercive field, energy product, for specific excitation conditions. Losses are also obtained from the major hysteresis loop measurement since they depend on the area of the loop. The $M(H)$ curve is the result of magnetization processes at the atomistic, domain and macroscopic level, which in turn depend on the underlying microstructure. Changes in temperature, frequency of the applied field or stress levels affect the $M(H)$ characteristic. The modeling of stress dependent magnetization processes is a challenging task due to the highly nonlinear dependence of the magnetization on external stimuli which is further complicated by the magneto-elastic coupling.

The stress-strain characteristic for any given material consists of an elastic region, where the stress is proportional to the strain and the proportionality constant is the Young's modulus, and a plastic region. The microstructure in plastically deformed materials consists of finer grains, hence longer grain boundaries acting as pinning centers, anisotropy dispersion, and magnetically hardened regions which considerably affect the magnetization response.

The long-term goal of our work is to develop a modeling approach that links stress-induced microstructural changes to the macroscopic parameters obtained from hysteresis loop or magnetic Barkhausen noise measurements [4], [12]. Towards this goal, in this paper, we report on the quasi-static micromagnetic modeling of the effect of microstructure on the major hysteresis loop phenomenology using the open source OOMMF software to minimize the free energy equation of material [12], [19].

The proposed methodology is presented in the following section which is followed by simulation results and their

¹Mehrija Hasičić is with the Faculty of Engineering and Natural Sciences, International Burch University, Francuske revolucije bb, 71000 Sarajevo, Bosnia and Herzegovina (e-mail: mehrija.hasicic@ibu.edu.ba), (<https://orcid.org/0000-0002-4679-3611>)

Aphrodite Ktena is with the Energy Systems Laboratory, National and Kapodistrian University of Athens, Evia, 34400, Greece (e-mail: apktena@uoa.gr), (<https://orcid.org/0000-0003-1350-2408>).

Jasna Hivziefendic is with the Faculty of Engineering and Natural Sciences, International Burch University, Francuske revolucije bb, 71000 Sarajevo, Bosnia and Herzegovina (e-mail: jasna.hivziefendic@ibu.edu.ba), (<https://orcid.org/0000-0002-0461-171X>)

discussion. The last section summarizes the main conclusions and presents the roadmap of our future work.

II. METHODOLOGY

In micromagnetic modeling, the minimization of the energy equation reflects the balance between long range and short-range interactions and their interplay with external stimuli, such as a magnetic field. Short range interactions have a localized effect and are determined by the competition between the exchange and anisotropy energy terms which reflect the effect of the chemical composition and the crystalline structure of the material. The long-range interactions are represented by the magnetostatic energy term which summarizes the magnetic fields experienced by a given elementary volume inside the material, as the former emanate from all the remaining volumes in it. This term depends on the current magnetic state of the material, which incorporates the effect of previous states as well, and is responsible for the hysteresis property observed in magnetic materials.

The effect of stress on the magnetization process was introduced through various microstructural configurations as well as through the parameters of anisotropy constant, exchange energy coefficient, and magnetic saturation which control the anisotropy, exchange and magnetostatic energy terms, respectively.

More details on micromagnetic calculations with OOMMF are given in [12] where the effect of simulation parameters on the major hysteresis loop phenomenology was studied. More specifically, we discussed the effect of discretization and cell size as well as the effect of magnetic parameters, such as the exchange and anisotropy constants and the orientation of the easy axis, on the major hysteresis loop.

In this work, we report on the effect of changes in microstructure through the introduction of hard magnetic inclusions in a soft matrix combined with changes in the direction of anisotropy, i.e. in the magnetic texture. The parameters used in the simulations to define different types of materials are the anisotropy coefficient K_1 , the exchange energy coefficient A_{ex} and the magnetic saturation M_s . The parameter values used in the simulation results shown here are summarized in Table I. They correspond to three different types of materials: Material 1 is homogeneous with parameters corresponding to a soft magnetic material, while Materials 2 and 3 have inclusions of hard material in the soft magnetic matrix. The inclusions of Material 3 are harder than those of Material 2 with parameters corresponding to those of a rare earth magnet.

TABLE I
MAGNETIC PROPERTIES OF MATERIALS

Material	Type of material	Parameters		
		K_1 [kJ/m ³]	A_{ex} [kJ/m]	M_s [kA/m]
Material 1	Soft	48	21	1700
Material 2	Hard	520	21	1400
Material 3	Hard	4500	21	1280

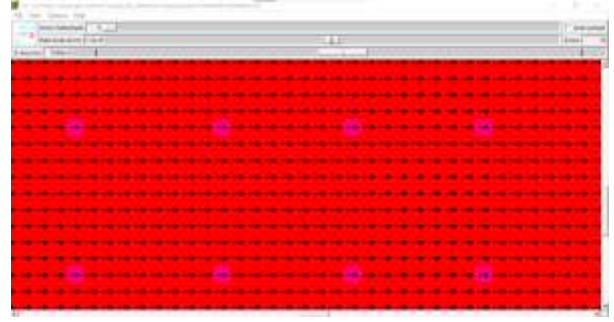


Fig. 1. shows the magnetization plot of a soft matrix with hard inclusions.

The simulated material is of rectangular shape discretized along the x (length), y (width) and z (thickness) direction in cubic cells of side a . The size of the cubic cells is a user defined variable which has to be chosen so that it is smaller than the magnetocrystalline exchange length for hard magnetic materials and magnetostatic exchange length for soft magnetic materials, as presented in [12]. Fig. 1 shows the initial state of the magnetization vector for every cell in the xy plane for a given z-value. The plot is zoomed in 35x so that it is easier to see the hard inclusions (in purple) which are of a size of one cell. The pattern continues throughout the sample in the xy plane. Simulations have been carried out for two cases, where hard inclusions are either cylindrical structures throughout the z layer, or one spherical cell in the middle z layer. Table II summarizes the texture and type of inclusions for the simulations shown here.

The applied field in all simulations is 1100 mT along the x-axis.

TABLE II
PROPERTIES OF HARD INCLUSIONS IN THE SOFT MATRIX USED IN THE SIMULATIONS

#	Hard inclusions	Anisotropy direction	Type of inclusions
1	Material 2	randomized	cylindrical
2	Material 2	[1 0 0]	cylindrical
3	Material 2	[0 1 0]	cylindrical
4	Material 2	[0 0 1]	cylindrical
5	Material 2	[1 1 0]	cylindrical
6	Material 2	[0 1 1]	cylindrical
7	Material 2	[1 0 1]	cylindrical
8	Material 2	[1 1 1]	cylindrical
9	Material 2	[1 0 0]	spherical
10	Material 2	[0 1 0]	spherical
11	Material 2	[0 0 1]	spherical
12	Material 2	[1 1 0]	spherical
13	Material 2	[0 1 1]	spherical
14	Material 2	[1 0 1]	spherical
15	Material 2	[1 1 1]	spherical
16	Material 3	[1 0 0]	cylindrical
17	Material 3	randomized	cylindrical

III. RESULTS

The base case used for comparison corresponds to a homogeneous magnetic material where all cells have the parameters of Material 1 and the anisotropy, saturation magnetization and the applied field are all along the x-axis or [1 0 0].

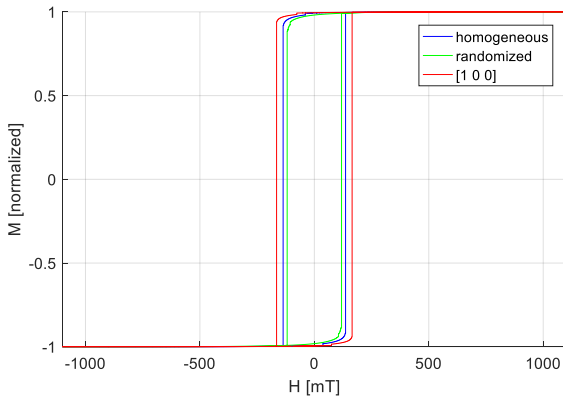


Fig. 2. Simulated hysteresis loops of a homogeneous magnetic material (blue) versus a material with cylindrical hard inclusions, extending throughout the z layer, with randomized anisotropy (green), and with the anisotropy oriented along the [1 0 0] (red) parallel to the applied field

First, we examine the effect of the anisotropy direction of hard magnetic inclusions of Material 2. In Fig. 2, the simulated hysteresis loop of the homogeneous case is compared against those of materials with cylindrical hard inclusions with anisotropy along the same direction as that of the soft matrix and the applied field, i.e. along [1 0 0], and with randomized anisotropy orientations. When the hard inclusions are aligned with the soft matrix, the coercivity increases as it is expected (red line). However, when the anisotropy of the inclusions is randomly dispersed, the material presents a softer response (green line). To better understand these results, we examine the energy plots for the two cases shown in Fig. 3.

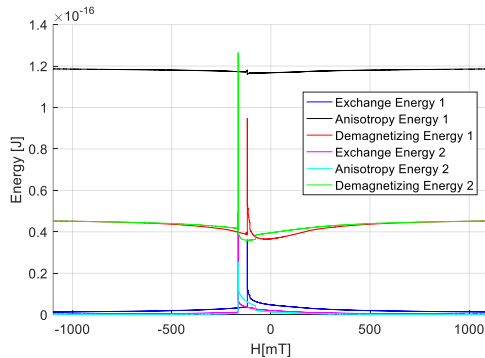


Fig. 3. Energy plots for materials with hard inclusions with randomized anisotropy (case 1) and anisotropy aligned with the anisotropy of the soft matrix (case 2)

The peak in the computed energy terms is observed around coercivity which is higher for the material with the hard inclusions along the same direction of the applied field (case 2). When the anisotropy is randomized (case 1), the anisotropy energy term is the most prominent and does not vary much with the field (black line). Exchange energy on the other hand is lower (blue line) even though the exchange constant used is the same in both cases. The exchange energy between two neighboring magnetic dipoles depends on the angle between their magnetization vectors, i.e. the larger the angle, the smaller the exchange energy. When the anisotropy is randomized and there is no predominant preferred direction, the resistance of a given magnetic volume to the forced change in magnetization is lower and the magnetization rotation towards the effective field experienced by the given volume is facilitated.

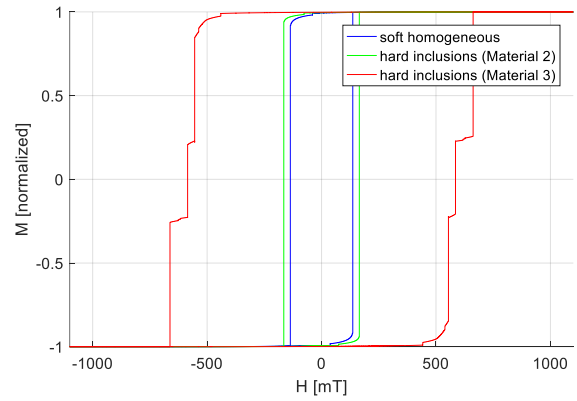


Fig. 4. Calculated hysteresis loops for the soft homogeneous case (blue) versus hard inclusions of Material 2 (green) and Material 3 (red)

The next step was to investigate the effect of magnetic hardness of the inclusions by carrying out simulations with inclusions of Material 2 and Material 3 (Fig. 4). The anisotropy and initial magnetization of hard inclusions in both samples is along [1 0 0]. The coercivity for the cases shown in Fig. 4 increases six-fold as the anisotropy constant of the inclusions increases almost ten-fold. Observed results are consistent with major hysteresis loop characteristics of harder magnetic materials. The step-like response of the loop corresponding to Material 3 (red line) is an artefact of the OOMMF calculation.

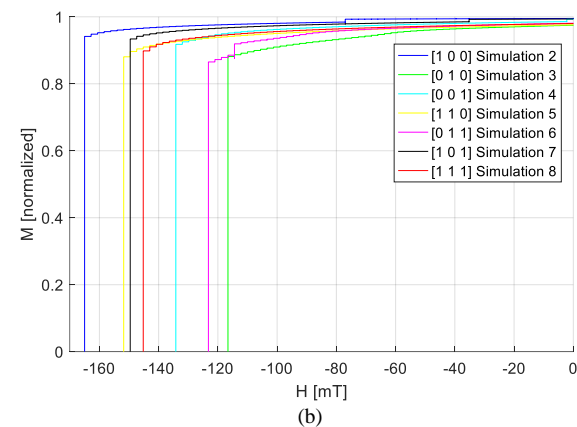
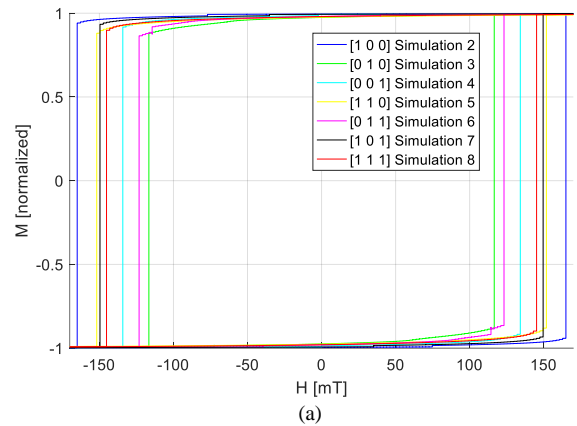


Fig. 5. Major hysteresis loop calculations for a sample with cylindrical hard inclusions of Material 2 throughout the z layer with the anisotropy lying along different directions (a) full loop (b) second quadrant

In Fig. 5 we present the effect of magnetic texture on the major hysteresis loop phenomenology of a sample with hard inclusions of Material 2. The details of each simulation are given in Table 2. The anisotropy direction is varied from

easy axis (x-axis) (#2) through various in-plane (#3 and #5) and out-of-plane (#4, #6, #7 and #8) directions.

Hard axis loops (#3 and #6) are narrower, as expected. The lowest coercivity is observed when the anisotropy is along y-axis [0 1 0] in-plane and along [0 1 1] direction, out of the plane, respectively. The case with the anisotropy pointing out of plane along [0 0 1] (#4) yields a higher coercivity than the previous cases. The widest loops are obtained when the anisotropy of the hard inclusions is along [1 0 0], collinear with the applied field, or has an x-component [1 1 0], [1 0 1] and [1 1 1] (#2, #5, #7 and #8).

The effect of distribution of hard cells along the z layer is investigated next, by arranging the hard inclusions only in one z layer, the middle one. The results are presented in Fig. 6.

Distributing the hard inclusions in only one z layer, while keeping the pattern along the xy plane presented in Fig. 1 consequently, means a decrease in the volume fraction of hard inclusions. Therefore, we observe that the widest major hysteresis loop presented in Fig. 6 is narrower than the widest major hysteresis loop presented in Fig. 5. The discussion of Fig. 5 is valid for Fig. 6 as well. The only different trend observed is that when the hard inclusions' anisotropy is along [0 1 0], the observed coercivity is 10 mT higher than in the case of cylindrical inclusions.

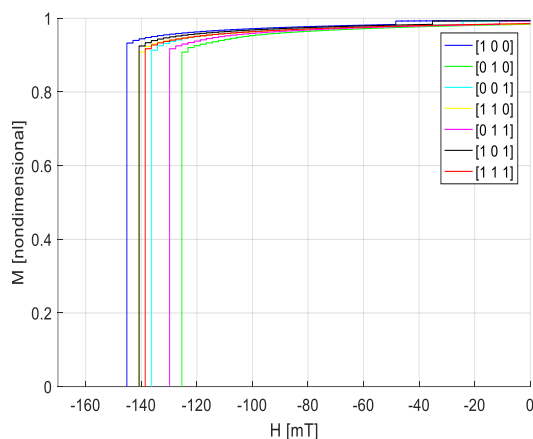


Fig. 6. Major hysteresis loop calculations for a sample with spherical hard inclusions of Material 2 in the middle z layer, with the anisotropy lying along different directions

The presented calculations demonstrate the effect of microstructure and magnetic texture on the observed phenomenology of the hysteresis loop. Experimental evidence has shown that both are affected in plastically deformed material [4], [20]. In our future work, simulations will be based on experimental measurements and the OOMMF software will be used to link microstructural parameters to macroscopic magnetic parameters obtained from a major hysteresis loop measurement, such as the differential permeability and coercivity which have a well-established dependence on residual stresses in a magnetic material.

The limitations of the OOMMF software, observed mainly in the approach to saturation in the third quadrant, need to be further examined and ensure that they do not affect the validity of our conclusions.

IV. CONCLUSION

The effect of microstructure and magnetic texture on the hysteresis loop has been studied through quasi-static micromagnetic simulations using the open-source software OOMMF. Microstructure was varied through cubic or columnar inclusions of different magnetic parameters inside a soft matrix. Magnetic texture was varied through the anisotropy orientation of the inclusions. Coercivity varies considerably with both microstructure and texture. When the hard inclusions have randomized anisotropy, lower coercivity is observed, even compared to the homogeneous case calculation. This is explained through the interplay between the different energy density terms, where the anisotropy energy density is predominant, and the exchange energy is reduced.

Future work will be focused on the correlation between simulation parameters and magnetic parameters obtained from measured loops at various residual stress levels on electrical sheet laminates.

REFERENCES

- [1] S. Banerjee and A. K. Tyagi, Eds., *Functional materials: preparation, processing and applications*, 1st ed. London; Waltham, MA: Elsevier, 2012.
- [2] K. Liang, S. Angelopoulos, A. Ktena, X. Bi, and E. Hristoforou, 'Residual Stress Distribution Monitoring and Rehabilitation in Ferromagnetic Steel Rods', *Sensors*, vol. 22, no. 4, p. 1491, Feb. 2022, doi: 10.3390/s22041491.
- [3] F. J. G. Landgraf, M. F. de Campos, and J. Leicht, 'Hysteresis loss subdivision', *Journal of Magnetism and Magnetic Materials*, vol. 320, no. 20, pp. 2494–2498, Oct. 2008, doi: 10.1016/j.jmmm.2008.04.003.
- [4] A. Ktena, M. Hasicic, F. J. G. Landgraf, E. Moudilou, S. Angelopoulos, and E. Hristoforou, 'On the use of differential permeability and magnetic Barkhausen Noise Measurements for Magnetic NDT Applications', *Journal of Magnetism and Magnetic Materials*, vol. 546, p. 168898, 2022, doi: https://doi.org/10.1016/j.jmmm.2021.168898.
- [5] E. C. Stoner and E. P. Wohlfarth, 'A mechanism of magnetic hysteresis in heterogeneous alloys', *Phil. Trans. R. Soc. Lond. A*, vol. 240, no. 826, pp. 599–642, May 1948, doi: 10.1098/rsta.1948.0007.
- [6] D. C. Jiles and D. L. Atherton, 'Theory of ferromagnetic hysteresis (invited)', *Journal of Applied Physics*, vol. 55, no. 6, pp. 2115–2120, Mar. 1984, doi: 10.1063/1.333582.
- [7] S. H. Charap and A. Ktena, 'Vector Preisach modeling (invited)', *Journal of Applied Physics*, vol. 73, no. 10, pp. 5818–5823, May 1993, doi: 10.1063/1.353538.
- [8] A. Ktena and E. Hristoforou, 'Stress Dependent Magnetization and Vector Preisach Modeling in Low Carbon Steels', *IEEE Transactions on Magnetics*, vol. 48, no. 4, pp. 1433–1436, Apr. 2012, doi: 10.1109/TMAG.2011.2172786.
- [9] T. Schrefl, J. Fidler, and H. Kronmüller, 'Nucleation fields of hard magnetic particles in 2D and 3D micromagnetic calculations', *Journal of Magnetism and Magnetic Materials*, vol. 138, no. 1, pp. 15–30, Nov. 1994, doi: 10.1016/0304-8853(94)90395-6.
- [10] J. Fidler and T. Schrefl, 'Micromagnetic modelling - the current state of the art', *J. Phys. D: Appl. Phys.*, vol. 33, no. 15, pp. R135–R156, Aug. 2000, doi: 10.1088/0022-3727/33/15/201.
- [11] W. Scholz *et al.*, 'Scalable parallel micromagnetic solvers for magnetic nanostructures', *Computational Materials Science*, vol. 28, no. 2, pp. 366–383, Oct. 2003, doi: 10.1016/S0927-0256(03)00119-8.
- [12] M. Hasičić and A. Ktena, 'Using OOMMF to Study the Effect of Microstructure on Magnetic Hysteresis Loops', in *Advanced Technologies, Systems, and Applications VI*, Cham, 2022, pp. 651–660.
- [13] D. C. Jiles, 'Hysteresis models: non-linear magnetism on length scales from the atomistic to the macroscopic', *Journal of Magnetism and Magnetic Materials*, vol. 242–245, pp. 116–124, Apr. 2002, doi: 10.1016/S0304-8853(01)02113-6.

- [14] B. Skubic, J. Hellsvik, L. Nordström, and O. Eriksson, 'A method for atomistic spin dynamics simulations: implementation and examples', *J. Phys.: Condens. Matter*, vol. 20, no. 31, p. 315203, Aug. 2008, doi: 10.1088/0953-8984/20/31/315203.
- [15] L. Daniel, M. Rekik, and O. Hubert, 'A multiscale model for magneto-elastic behaviour including hysteresis effects', *Arch Appl Mech*, vol. 84, no. 9, pp. 1307–1323, Oct. 2014, doi: 10.1007/s00419-014-0863-9.
- [16] L. DANIEL, L. Bernard, and O. Hubert, 'Multiscale Modeling of Magnetic Materials', in *Reference Module in Materials Science and Materials Engineering*, Elsevier, 2020. doi: 10.1016/B978-0-12-803581-8.12056-9.
- [17] W. Zhao, S. Wang, X. Xie, X. Zhou, and L. Liu, 'A simplified multiscale magneto-mechanical model for magnetic materials', *Journal of Magnetism and Magnetic Materials*, vol. 526, p. 167695, May 2021, doi: 10.1016/j.jmmm.2020.167695.
- [18] P. Fagan, B. Ducharme, L. Daniel, and A. Skarlatos, 'Multiscale modelling of the magnetic Barkhausen noise energy cycles', *Journal of Magnetism and Magnetic Materials*, vol. 517, p. 167395, Jan. 2021, doi: 10.1016/j.jmmm.2020.167395.
- [19] M. J. Donahue and D. G. Porter, *OOMMF Documentation*. National Institute of Standards and Technology. Accessed: Oct. 26, 2020. [Online]. Available: <https://math.nist.gov/oommf/doc/userguide20a2/userguide/>
- [20] F. J. G. Landgraf, M. Emura, K. Ito, and P. S. G. Carvalho, 'Effect of plastic deformation on the magnetic properties of non-oriented electrical steels', *Journal of Magnetism and Magnetic Materials*, vol. 215–216, pp. 94–96, Jun. 2000, doi: 10.1016/S0304-8853(00)00075-5.